

# RSC Advances



This is an *Accepted Manuscript*, which has been through the Royal Society of Chemistry peer review process and has been accepted for publication.

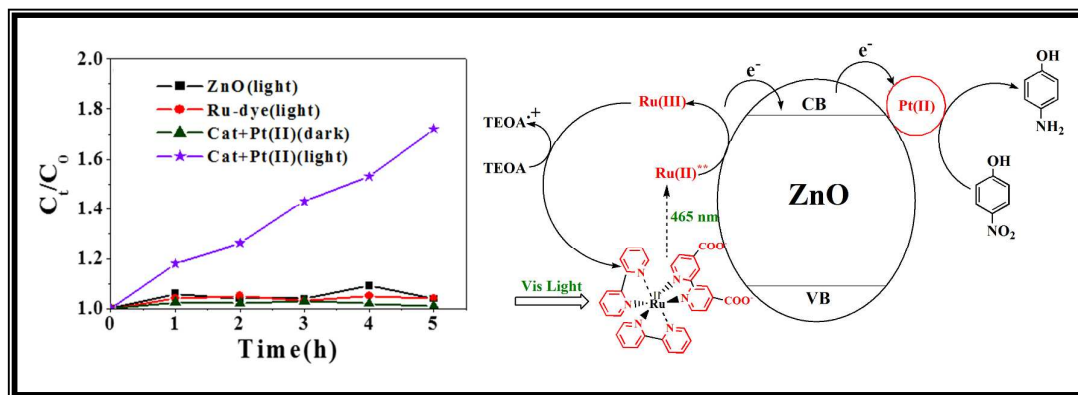
*Accepted Manuscripts* are published online shortly after acceptance, before technical editing, formatting and proof reading. Using this free service, authors can make their results available to the community, in citable form, before we publish the edited article. This *Accepted Manuscript* will be replaced by the edited, formatted and paginated article as soon as this is available.

You can find more information about *Accepted Manuscripts* in the [Information for Authors](#).

Please note that technical editing may introduce minor changes to the text and/or graphics, which may alter content. The journal's standard [Terms & Conditions](#) and the [Ethical guidelines](#) still apply. In no event shall the Royal Society of Chemistry be held responsible for any errors or omissions in this *Accepted Manuscript* or any consequences arising from the use of any information it contains.

## Graphical Abstract

Utilization of Ru(II)-complex immobilized ZnO hybrid in presence of Pt(II) co-catalyst for photocatalytic reduction of 4-nitrophenol under visible light



Cite this: DOI: 10.1039/c0xx00000x

www.rsc.org/xxxxxx

## Paper

**Utilization of Ru(II)-complex immobilized ZnO hybrid in presence of Pt(II) co-catalyst for photocatalytic reduction of 4-nitrophenol under visible light**

Sumana Bhar, Rajakumar Ananthkrishnan\*

Received (in XXX, XXX) Xth XXXXXXXXXX 20XX, Accepted Xth XXXXXXXXXX 20XX  
DOI: 10.1039/b000000x

In this present study, an attempt has been made to utilize the Ru-dye sensitized ZnO hybrid along with Pt(II) salt for the visible light aided photoreduction of 4-nitrophenol. The dye, Bis(2,2'-bipyridyl)(4,4'-dicarboxy-2,2'-bipyridyl)ruthenium(II) chloride, is used as a sensitizer to ZnO. The photocatalyst, Ru dye-ZnO, is characterized by XRD, FTIR, DRS, SEM, EDX and XPS. The kinetic study of the photoreduction reaction is carried out under visible light irradiation (CFL 45W) with different concentrations of Pt(II) ions without changing the 4-nitrophenol concentration. The percentage reduction is reached a maximum of 55-60% in presence of  $2.5 \times 10^{-4}$  mol% Pt(II) salt concentration. Control studies are done (in the presence of light and dark) to establish the photoactivity of the prepared photocatalyst. A series of experiments is conducted to understand the mechanistic view of the photo-reduction process, and it is identified that photoreduction of 4-nitrophenol is going through an electron transfer process.

**Introduction**

In recent decades, potentially hazardous contaminants in waste water or ground water are treated or reduced by photolysis under artificial light irradiation or solar light irradiation.<sup>1</sup> However, many pollutants due to their low light absorptivity or due to the low quantum yield of the photoreaction, are not susceptible to photodegradation or photoreduction or any photochemical reaction. In those cases, a photoactive substance can be added deliberately to facilitate the reaction in the forward direction. Most of the research works in the past, photodegradation or photoreduction of pollutants were performed using wide band gap semiconductors, such as,  $\text{TiO}_2$ ,<sup>2, 3</sup>  $\text{ZnO}$ ,<sup>4, 5</sup> and  $\text{SnO}_2$ <sup>6</sup> under UV light irradiation. Since the UV spectrum, which is needed to excite these wide band gap semiconductors, covers only less than 5% in the solar spectrum reaching the surface of the earth. Again handling the UV light is disadvantageous due to its hazardous nature as well as its cost of generation. Therefore, researchers are interested to find materials to utilize the cost effective visible light for water treatment and photochemical processes. In order to utilize the visible light from solar energy, and enhance the energy conversion efficiency during the photocatalytic reaction, researches have involved in the modification of wide band gap semiconductor to absorb light in the visible region. Among these methods, metal doping<sup>7, 8</sup> and photosensitization<sup>9</sup> are widely used as inexpensive methods to excite the semiconductors using the visible light. Introducing defect or oxygen vacancy in the metal oxide is also another interesting way of making it as a visible light active material.<sup>10</sup> Photosensitization can be achieved by a

photosensitizer adsorbed on semiconductor surface, absorbs light energy, transforms the light energy to chemical energy and transfers it under favourable conditions to photochemically unreactive substrates.<sup>11</sup> The most studied visible light photosensitizers are various organic dyes, such as eosin-Y,<sup>12</sup> rose bengal,<sup>13</sup> riboflavin,<sup>11, 13, 14</sup> Inorganic metal complexes<sup>15, 16</sup> or Inorganic sensitizer<sup>17</sup> etc. Sensitizer usually absorbing light gets excited and injects an electron into the conduction band of the semiconductor.<sup>18</sup>

The majority of the dye sensitized photocatalysis reactions are based on dye sensitized  $\text{TiO}_2$  catalyst.<sup>15, 19</sup> However, ZnO has similar band gaps to that of  $\text{TiO}_2$  and also possess higher electron mobility than the  $\text{TiO}_2$ .<sup>20</sup> Hence, it can be utilized as an alternate to the  $\text{TiO}_2$  in dye sensitized photocatalytic reactions. Several attempts have been made previously to utilize the dye sensitized ZnO in photocatalytic removal of Cr(VI),<sup>21</sup> photodegradation of Methylene Blue dye in water.<sup>22</sup> In this study we focus on dye sensitized ZnO based hybrid for the visible light photocatalysis.

In the recent decades, nitro compounds are widely produced in the industrial process as by-products, and nitrophenols are hazardous to the environment. Again, hydrogenation of nitroaromatics to corresponding amines is an important organic transformation practised in industries. Aminophenols are widely exploited as precursors in the manufacturing process of variety of medicines, like paracetamol, acetanilide, phenacetin, etc. Traditional reduction method adopts environmentally dangerous chemicals and result in undesirable toxic metal sludge. Recently, developments have taken place in greener (photochemical) methodologies for reduction or degradation of nitrogenous organics under the solar light. However, the nitrophenol is known

to be photoresistive and stable under the sun light.<sup>3</sup> Literature reports indicate that photoreduction of nitro compounds usually carried out using various semiconductor photocatalysts like TiO<sub>2</sub>,<sup>23</sup> CdS,<sup>24, 25</sup> ZnO, graphene modified CdS quantum dots,<sup>26</sup> Au doped CdS,<sup>27</sup> Ag(0) modified TiO<sub>2</sub><sup>28</sup> etc. Our group has previously reported the visible light aided photocatalytic reduction of 4-nitrophenol in a metal free green condition using resin supported eosin-Y as a visible light active photocatalyst.<sup>29</sup> Ru-dye sensitized ZnO has been widely used for solar cell application.<sup>30</sup> But its photocatalytic activity in various types of organic transformation reactions, under visible light irradiation is yet to be explored. In the present study, a Ru(II)-dye immobilized ZnO hybrid in presence of Pt(II) ions (as a co-catalyst) has been used for the first time to carry out photoreduction of nitrophenol under the visible light. The results of photocatalytic studies under different conditions including control studies for understanding mechanism are described here in detail.

## Results and Discussions

There are many organic dyes which have been previously used for sensitizer for wide band gap semiconductors.<sup>11-14</sup> Here the dye selected for sensitization of ZnO is ruthenium based, Bis(2,2'-bipyridyl)-(4,4'-dicarboxy-2,2'-bipyridyl)ruthenium(II) chloride ([Ru(bpy)<sub>2</sub>(dcbpy)]Cl<sub>2</sub>). The carboxylic groups are introduced in one of the bipyridyl moieties, by oxidizing the methyl derivative of bipyridyl ligand<sup>31</sup> to facilitate bonding of the complex with ZnO. The present choice is advantageous over [Ru(dcbpy)<sub>3</sub>]<sup>2+</sup>, since six peripheral carboxyl groups would be able to bind the multiple nanoparticles which will lead aggregation of photocatalyst.<sup>32</sup> The aggregation process would not be preferable for photocatalytic systems. The dye selected in our study has the much higher photochemical and photo-redox stability than that of most of the organic dyes given that in acetonitrile solution the single exponential emission lifetime of Ru(bpy)<sub>2</sub>(dcbpy)<sup>2+</sup> MLCT state is 490 ns (0.5 μs).<sup>34</sup>

### Characterization of the hybrid photocatalyst

The prepared hybrid material was characterized by various techniques to understand its photo-activity and surface properties. The catalyst was subjected to the characterization by X-Ray diffraction analysis, FT-IR spectroscopy, Diffuse Reflectance Spectroscopy, Secondary Electron Microscopy (SEM), Energy Dispersive X-Ray Analysis (EDX) and X-Ray Photoelectron Spectroscopy (XPS). Spectral studies were verified using a double beam UV-Visible Spectrophotometer (Thermo Scientific Evolution 201 UV-Visible Spectrophotometer).

### XRD analysis

XRD data of the hybrid photocatalyst was obtained using Bruker Apex-2 X-Ray diffractometer. The XRD pattern of the catalyst system (Fig. 1a) showed a similar peak pattern to that of unmodified ZnO. The planes were indexed in the figure, which indicated there was no new phase formation occurring during the sensitization process.

### XPS studies

The XPS spectrum of the hybrid photocatalyst, obtained from PHI 5000 Versa Probe II using crystal colloidal monochromator,

showed a doublet centered at 1020 eV and 1043 eV corresponding to Zn2p<sub>3/2</sub> and Zn2p<sub>1/2</sub> core levels (Fig. 1b).<sup>33a</sup> A sharp peak centre at 530 eV in the spectrum corresponds to the O1s<sub>1/2</sub> level originating from bulk oxygen. A small peak appeared at 280 eV, which corresponds to Ru3d<sub>5/2</sub> core level. Hence, it revealed that the immobilization of Ru-dye sensitizer had occurred over ZnO surface.

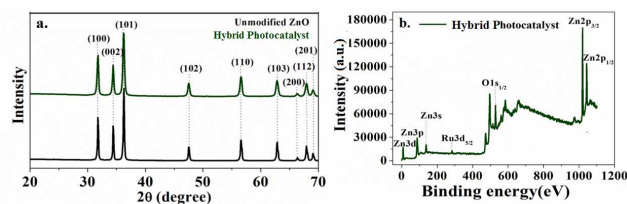
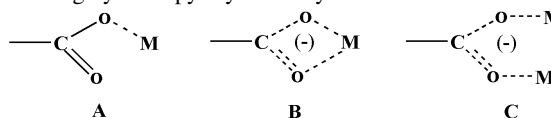


Figure 1: (a) XRD spectrum of photocatalyst and unmodified ZnO (Intensity in arbitrary unit), (b) XPS spectrum of photocatalyst.

### FTIR studies

FTIR spectra of the photocatalyst and the dye were recorded by Perkin Elmer FTIR Spectrophotometer RXI. The spectrum (Fig. 2(a)) showed the sharp peaks at 3432 cm<sup>-1</sup>, 2375 cm<sup>-1</sup>, 1625 cm<sup>-1</sup>, 1393 cm<sup>-1</sup> and 542 cm<sup>-1</sup>. The peaks at 3432 cm<sup>-1</sup> and 542 cm<sup>-1</sup> are assigned to O–H stretching frequency on the ZnO surface and Zn–O stretching mode respectively. The peaks at 1535 cm<sup>-1</sup> and 1393 cm<sup>-1</sup> are due to C–O asymmetric stretching of the carboxylic groups in the photocatalyst, showed a blue shift from their original 1630 cm<sup>-1</sup> and 1445 cm<sup>-1</sup> values in the [Ru(bpy)<sub>2</sub>(dcbpy)]Cl<sub>2</sub> dye. This indicated that the dye bounded to the ZnO surface through carboxylic acid terminal. The exact binding nature between the dye and Zn centre is still unknown. One common method of binding between the Ru-polypyridyl complex and metal oxide involves the dehydrative covalent bonding by the bipyridyl carboxylic acids to the oxide surface.



Scheme 1: Probable binding mode of Ru-dye to the metal centre.

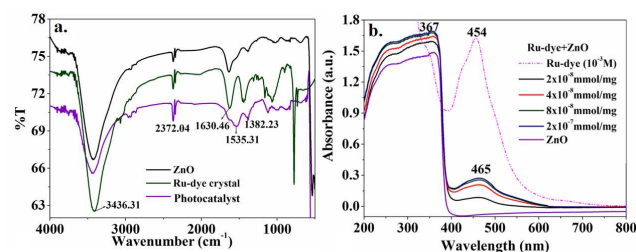
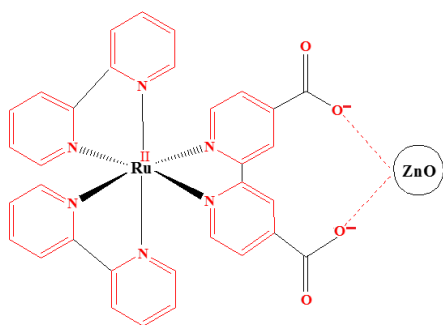


Figure 2: (a) FTIR spectra of ZnO, Ru(II) metal complex and the photocatalyst, (b) DRS spectra of ZnO and the photocatalyst with different dye loading and UV-Vis spectrum of Ru(II) metal complex.

The carboxylate group can bind to the metal centre in different modes. Among these, an ester linkage has two non-equivalent C–O bond and expected to show a higher energy ν value in case of (A) in scheme 1. The peak at 1535 cm<sup>-1</sup> is assigned to ν (COO<sup>-</sup>) possibly for (B) and (C) in scheme-1.<sup>33b,c</sup>



Scheme 2: A schematic diagram of Ru(II) metal complex on ZnO surface.

### Diffuse reflectance spectroscopic analysis

DRS spectrum of the photocatalyst was recorded by CARY 5000 UV-Vis-NIR spectrophotometer. The spectra in Fig. 2(b) showed a sharp absorption peak at 367 nm, which is due to the characteristic absorption of ZnO, along with a new peak at 465 nm due to the absorption of dye molecule. This again confirmed the binding of dye molecule on ZnO surface. The absorption in the visible region suggested that the photocatalyst might be used under visible light condition. The ethanolic solution of [Ru(bpy)<sub>2</sub>(dcbpy)]Cl<sub>2</sub> dye showed the characteristic MLCT peak at 454 nm (Fig. 2(b)). But after binding on ZnO surface, the absorption peak red shifted to 465 nm.<sup>34</sup> When the dye concentration was increased, the absorbance intensity at 465 nm was also increased with a saturation limit of 8x10<sup>-8</sup> mmol/mg - 2x10<sup>-7</sup> mmol/mg of dye concentration.

### Scanning electron microscopic studies

Since the catalysis occurs on the surface of the photocatalyst, the nature of the surface of the photocatalyst is a matter of importance. SEM image, obtained from Supra 40, Carl Zeiss instrument, in Fig. 3(a) of the photocatalyst showed the dispersive nature of the photocatalyst surface. The surface structure of the adsorbed dye depends on various factors like sensitization time and the concentration of dye. With the increasing concentration of dye and the sensitization time the dye sensitized photocatalyst tends to agglomerate.<sup>20, 35</sup> which may not be a favourable condition for any photocatalytic reaction. Hence, we have used milder conditions of dye concentration 8x10<sup>-8</sup> mmol/mg and an optimum time limit of 12 h, to avoid aggregation of surfaces. The EDX spectrum of the photocatalyst showed the peaks of Ru along with Zn and O, which further confirmed the dye binding on ZnO surface (Fig. 3 (c)).

### Application of the prepared hybrid

In order to find the catalytic activity of the photocatalyst under visible light irradiation, photo-oxidative degradation and photoreduction of 4-nitrophenol were investigated. The kinetics of the reactions was analyzed by UV-Vis spectra of the aliquot taken in a regular interval of time. The neutral 4-nitrophenol absorbs light at 317 nm. On addition of TEOA of concentration 2x10<sup>-4</sup> M, 4-nitrophenol partially ionizes to 4-nitrophenolate ion

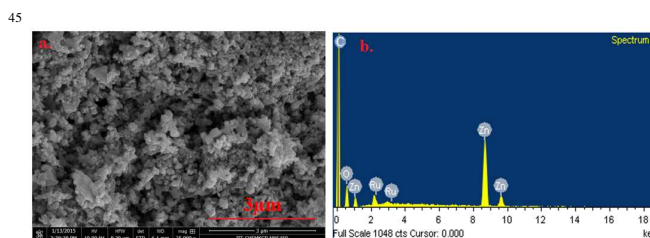


Figure 3: (a) SEM image of the photocatalyst showing dispersive nature, (b) EDX spectrum of photocatalyst.

imparting a pale yellow colour in the solution corresponding  $\lambda_{\text{max}}$  value at 400 nm. For the complete ionization of 4-nitrophenol in the aliquot solution, a necessary amount of 1M TEOA solution was added to the aliquot solution, which helped the separation of the absorption peak of 4-nitrophenol (317 nm) from that of 4-aminophenol (300 nm). The spectral curve of the aliquot solution showed a gradual decrease in the absorption intensity of the peak at 400 nm corresponding to the 4-nitrophenolate ion and a new peak appeared at 300 nm with increasing intensity with time. The new peak at 300 nm is due to the 4-aminophenol generated from the reduction of 4-nitrophenol under visible light irradiation with time.<sup>29, 36</sup> According to Beer's law,

$$A = \epsilon cl,$$

where, A = absorbance of the species,  $\epsilon$  = absorption coefficient of the species, c = concentration of the species in solution, l = path length in cm.

Since, the absorbance value of 4-nitrophenol at any moment during the reaction is directly proportional to the concentration of the 4-nitrophenol present in the solution, the same is also true for 4-aminophenol generated in the medium. Therefore, the ratio of absorbance value at any time 't' and the initial absorbance value ( $t = 0$  h) should be equal to the ratio of the concentration of 4-aminophenol (i.e.,  $A_t/A_0 = C_t/C_0$ ). So the kinetic of the reaction was investigated by monitoring the increase in intensity of the peak at 300 nm corresponding to 4-aminophenol using UV-Vis absorption spectroscopy.<sup>37</sup> The kinetic of the reduction reaction was also monitored by HPLC recorded by Thermo Scientific Dionex Ultimate 3000 with Diode Array Detector (supporting information Fig. S5). The spectra showed a gradual decrease in 4-nitrophenol peak.

### Adsorption of 4-nitrophenol on catalyst surface

Adsorption of the reactant on the surface of the catalyst is a first important step to consider in any heterogeneous catalysis reaction. In this study, the 4-nitrophenol solution was stirred with the necessary amount of catalyst and catalytic amount of Pt(II) salt in the dark.

An aliquot was taken out in every 15 min and further analyzed by UV-Visible spectrometer. The result showed that there was a decrease in 4-nitrophenol absorption peak indicating adsorption of 4-nitrophenol on the catalyst surface. After 45 min the spectral data suggested that the adsorption-desorption equilibrium between catalyst and 4-nitrophenol has reached. Therefore, before every catalysis reaction, the reaction mixture was stirred with the catalyst for 60 min in the dark.

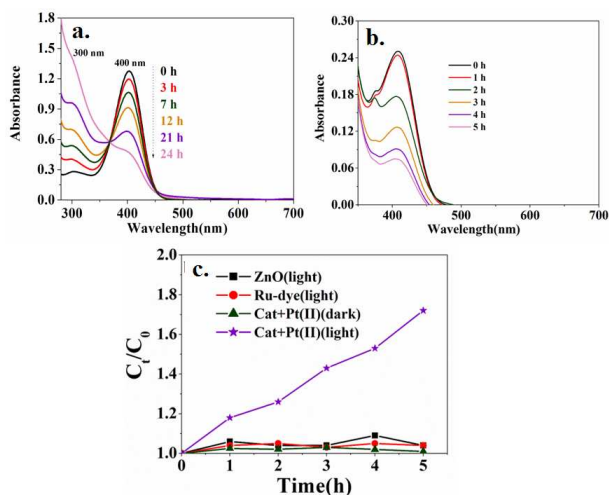


Figure 4: (a) UV spectra of the photo-reduction reaction showing a decrease in absorbance value at 400 nm and increment in 300 nm with time. (b) UV spectra of the oxidative photo-degradation of 4-nitrophenol (2 ppm). (c) Controlled studies with different components and catalyst in dark for 5h

### Effects of various parameters on the photoreduction of 4-nitrophenol

A series of kinetic experiments of the photoreduction of 4-nitrophenol was done in order to identify the effect of various parameters on photoreduction (Fig. 4(c)). The kinetic study was also carried out in the absence of light irradiation for 5 hour. The result showed no new peak at 300 nm appeared with time in the dark reaction, therefore, indicated the necessity of the visible light for the reduction process. Control kinetic study was performed on each separate component of the prepared photocatalyst along with a catalytic amount of Pt(II) salt using the sample experimental conditions under the visible light. Results indicated that there was no significant change in reaction mixture, i.e., neither any decrease in the absorbance intensity of 4-nitrophenolate ion (400 nm peak) nor any new peak at 300 nm (aminophenol) was observed. Meanwhile, experiment was conducted with the catalyst alone condition, where the 4-nitrophenol showed an oxidative degradation under the visible light irradiation (Fig. 4(b)). For the 2 ppm concentration of 4-nitrophenol, a 70% photo-oxidative degradation was observed. The percentage degradation was measured by analysing the decrease in absorbance value at 400 nm corresponding to the 4-nitrophenol.

The variation of the amount of Pt(II) salt in the reaction mixture was experimented to observe its effect on the photoreduction kinetics (Fig. 5(b)). The concentration of Pt(II) was varied from  $1 \times 10^{-4}$  to  $10 \times 10^{-4}$  mol%. It was observed that the reaction rate had increased with the increasing Pt(II) concentration to an optimum value of  $2.5 \times 10^{-4}$  mol% of Pt(II) concentration, and then decreased significantly with the increasing Pt(II) concentration. It is reported in literature that the photocatalytic activity depends on the oxidation state of the platinum source and followed the order Pt (clusters) > Pt(II) >> Pt(IV) as explained by Remita et al.<sup>8</sup> It can be assumed that with the increasing concentration of Pt(II) in the reaction mixture, the positively charged Pt(II) ions make an attractive scavenger for the photogenerated electrons instead of shuttling them to the

substrate. During the reaction, the Pt(II) ions got adsorbed on the surface of catalyst forming clusters.<sup>8, 16</sup> The XPS of the catalyst after the reaction (supporting information Fig. S2) showed the presence of Pt (peak at 72 eV) which supported our proposition. Again, the photocatalytic activity of the Pt(0) species depends on their preparation. The reduction of Pt(IV) to Pt(0) nanoparticles produces less active catalyst.<sup>16</sup>

All the kinetic experiments were carried out with the photocatalyst system of maximum dye loading since from DRS spectra of the photocatalyst of different dye loading showed maximum absorption for dye loading ( $8 \times 10^{-8}$  mmol/mg). Variation of dose of catalyst was also done to demonstrate its effect on the photoreduction. The catalytic amount was varied from 0.5 g/L to 1.25 g/L (Fig. 5(a)). Results showed a steady increase in photo-conversion to an optimum saturation of 55 – 60% in 1 g/L – 1.25 g/L of catalyst. It is quite obvious that the increasing amount of catalyst offers more catalytic surface favourable for the reaction to occur faster.

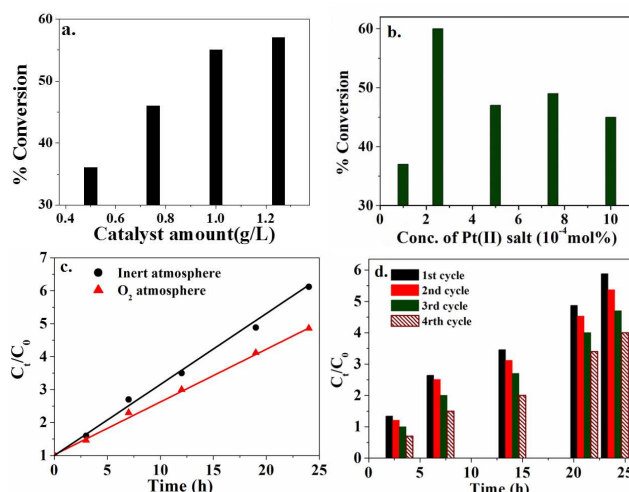


Figure 5: Photo-reduction reaction in various conditions, (a) Variation of catalytic amount, (b) variation of Pt(II) salt in the photo-reduction, (c) photo-reduction reaction in different atmosphere, (d) Catalyst recyclability test for four cycle

The photoreduction reaction was carried out in presence of various sacrificial donors like triethyl amine (TEA), di-isopropyl amine (DIPA), and diethanol amine (DEA). Surprisingly, the percentage conversion of the 4-nitrophenol increased significantly in presence of TEA (supporting information S3). It was therefore, concluded that the presence of water in the commercially available TEA helped the photocatalytic reduction by acting as a source of proton. In order to support this proposition we carried out the photoreduction reaction in presence of distilled TEA and found that the percentage conversion was significantly lesser than the previous case.

The catalytic reaction was done in presence of Ni<sup>2+</sup> and Pd<sup>2+</sup> instead of Pt<sup>2+</sup> ions. There was no reduction of 4-nitrophenol observed in case of Ni<sup>2+</sup> ions whereas in presence Pd<sup>2+</sup> ions reduction of 4-nitrophenol was observed with the deposition of black nanoparticle of Pd in reaction medium.

The reusability test of the photocatalyst was done in multiple times in presence of a catalytic amount of Pt(II) salt (Fig. 5(d)). The data showed that the catalyst can be reusable after 2nd and

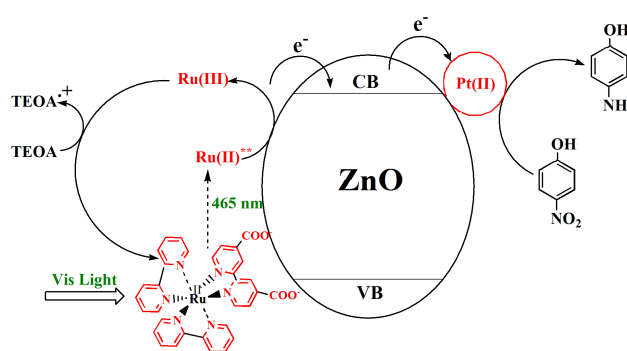
3rd cycle also. The loss of activity observed after fourth cycle, can be attributed to the fact the leaching out of the dye from the catalyst surface.

### 5 Mechanism Investigation

In this present study, the commercial ZnO was sensitized by immobilizing Ru-metal complex on the surface of metal oxide, which absorbs green light (465 nm), i.e., the region with highest intensity in the solar spectrum.<sup>16</sup> The kinetic study of photoreduction of 4-nitrophenol was done in presence of 10% benzoquinone solution, which is a known superoxide radical quencher.<sup>38</sup> The result showed no hindrance in the reaction rate, which confirmed that the present reaction was not governed by radical pathway. Since the photocatalytic system is based on a sensitization process, therefore, the sensitization theory can be significantly applicable to our system.<sup>11</sup> Based on this, the Ru-dye when irradiated under visible light, absorbs green light and gets excited and forms excited singlet. It undergoes inter-system crossing (ISC) to form stable triplet.<sup>39</sup> The excited dye molecule injects electrons into the conduction band of ZnO.<sup>34, 40</sup> Those electrons are transferred to Pt(II) surface, which produces H<sub>2</sub> by abstracting one proton from the sacrificial donor which facilitates the reduction of 4-nitrophenol.<sup>16, 41</sup> The catalytic cycle is closed by the sacrificial donor, TEOA, which reduces the Ru(III) to its initial Ru(II) state. The overall details are depicted in the Scheme 3.

In a photocatalytic reaction, the noble metal has the role of storing and mediating the photo-generated electrons from the semiconductor to an acceptor which is to be reduced.<sup>42</sup> Therefore, the photocatalytic reaction was carried out in presence of an electron acceptor molecular O<sub>2</sub> (Fig. 5(c)). The result showed a decrease in photoreduction reaction rate in presence of O<sub>2</sub> environment. Generally, in a photocatalytic degradation reaction by dye sensitized semiconductor system involves photo-generated electron first transfers from excited dye to the semiconductor conduction band which reduces molecular O<sub>2</sub> to form superoxide radical (O<sub>2</sub><sup>•-</sup>). The superoxide radical (O<sub>2</sub><sup>•-</sup>) eventually may form hydroxyl radical reacting with the solvent,<sup>15, 22</sup> which are the active species for degradation of organic pollutants. Earlier our group has reported Ru(bpy)<sub>3</sub><sup>2+</sup> aided synthesis of aryl pyridine in a homogeneous medium in which superoxide radical (O<sub>2</sub><sup>•-</sup>) is operative during the photo-conversion process. Therefore, in presence of molecular O<sub>2</sub> the reduction of 4-nitrophenol gets hindered as formation of radicals occurs through reduction of molecular O<sub>2</sub> which may help in the degradation of 4-nitrophenol but not in its reduction to 4-aminophenol.

The XPS study of the catalyst after reaction showed the peak of Pt 4f<sub>7/2</sub> core level (Supporting information Fig. S2) which indicated that the Pt(II) ions deposited on catalyst surface during the course of reaction forming cluster over the catalyst. The DRS study of catalyst after use (supporting information Fig. S1) also showed a red shift from its original value (465 nm to 490 nm) suggesting the inclusion of Pt(II) ions on the catalyst surface.



Scheme 3: A schematic diagram to express the plausible mechanism for the photo-reduction of 4-nitrophenol.

### 60 Effect of pH

The pH of the reaction mixture was measured as 8.0, which was due to the addition of sacrificial donor TEOA. Importantly, the pH stability domain of ZnO is narrower. Hence, ZnO can be dissolved under the acidic conditions of the reaction, resulting in the formation of Zn<sup>2+</sup>/dye agglomerates that absorb the incoming light but do not participate in the photocatalysis reaction.<sup>20, 35</sup> Again in more basic condition ZnO can be hydrolysed (pH>10), which would destroy the photocatalytic system. So it is favourable to do the photoreduction reaction in a optimised pH between 7-9.

### GCMS Study

In order to find the reduction product of 4-nitrophenol, the GCMS of reaction mixture was recorded. The MS spectrum (Fig. 6) of the reduced product after 24 h reaction showed the peak of 4-aminophenol (m/z = 109.10) and unreacted 4-nitrophenol (m/z = 139.08) and their fragmented products like phenol (m/z = 94.13), aniline (m/z = 93.12), benzene (m/z = 77.15), 1,3-butadiene (m/z = 53.09).

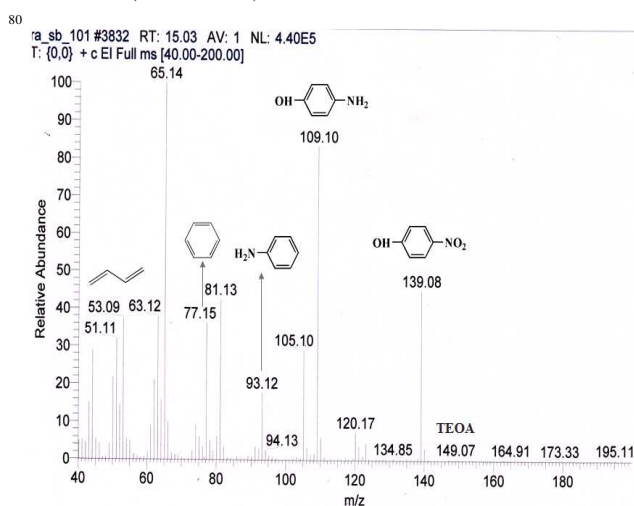


Figure 6: GCMS Spectrum of the reduction product after 24 h reaction.

In summary, the hybrid material was successfully used as a catalyst for photoreduction of 4-nitrophenol to 4-aminophenol in presence of Pt(II) and Pd(II) metal salt as a co-catalyst. The reduction reaction was optimised using 1 g/L catalyst in 10 ppm of 4-nitrophenol solution in presence of 2x10<sup>-4</sup> M TEOA solution. The co-catalyst was used in the catalytic amount (2.5 x 10<sup>-4</sup> mol

%). The %conversion value was calculated from calibration curve of 4-nitrophenol in 0.25M TEOA solution (supporting information Fig. S4).

## 5 Conclusion

In this study, ZnO, a UV absorbing material, has been successfully modified into a visible light active hybrid photocatalyst by immobilizing with the Ru(II) dye sensitizer (Bis(2,2'-bipyridyl)-(4,4'-dicarboxy-2,2'-bipyridyl)ruthanium(II) Chloride). The prepared hybrid has been utilized as a heterogeneous photocatalyst for the photo-reduction of 4-nitrophenol into 4-aminophenol. Control studies were carried out to identify the role of the visible light, sacrificial donor, basicity of the medium, and radical formation, in the present photoreduction process. The optimized condition for the effective photoreduction of 4-nitrophenol was arrived. The effective conversion of 4-nitrophenol (10 ppm) in  $2 \times 10^{-4}$  M TEOA solution is 55-60% in 24 h. From our mechanistic study, it was arrived that the photoreduction process was taking place through an electron transfer pathway. Moreover, the photocatalyst was found to be recyclable for repeated usage (minimum three times) and effective under the visible light condition.

## Experimental Section

The chemicals, which were used for the preparation of metal complex and the photocatalyst, were of analytical grade and have been used without further purification. The metal salt  $\text{RuCl}_3 \cdot 3\text{H}_2\text{O}$ , the ligands 2,2'-bipyridine and 4,4'-dimethyl-2,2'-bipyridine were bought from Spectrochem and Alfa Aesar, respectively. Nano-sized ZnO was obtained from Alfa Aesar.

### Preparation of $[\text{Ru}(\text{bpy})_2(\text{dcbpy})]\text{Cl}_2$ metal complex:

The carboxylic derivative of ligand 4,4'-dimethyl-2,2'-bipyridine was obtained by  $\text{KMnO}_4$  oxidation process as described in literature.<sup>31</sup> The Ru-metal complex was prepared as follows:<sup>44</sup> the metal salt  $\text{RuCl}_3 \cdot x\text{H}_2\text{O}$  (0.5 mmol), 2,2'-bipyridine (1 mmol) and 4,4'-dicarboxy-2,2'-bipyridine (0.5 mmol) were dissolved in water. Freshly prepared sodium phosphinate solution was added drop-wise to the reaction mixture and then heated to boil for 30 min. During the reflux, the initial green colour of the solution changed to a deep red. The solution was then filtered and the filtrate was mixed with KCl (0.05 mol) solution. The solution containing the crude product was now heated to boiling for a few minutes to get a deep red solution, which on cooling to room temperature yielded beautiful, red, plate-like crystals. These crystals were filtered, washed with ice-cold 10% aqueous acetone and then with acetone, and air dried. The yield of the complex was 70%.

### 50 Preparation of the photocatalyst:

A suspension of the dye  $[\text{Ru}(\text{bpy})_2(\text{dcbpy})]^{2+}$  ( $2 \times 10^{-4}$  M) and an appropriate amount of ZnO (1 g, 0.5 g, 0.25 g) in acetonitrile was stirred for 12 h in room temperature (303K). The resulting solid was washed several times in acetonitrile and dried in an oven. The solid obtained was directly used in the photoreduction process along with a catalytic amount of  $\text{K}_2\text{Pt}^{\text{II}}\text{Cl}_4$  salt.

### Photoreduction reaction:

A 10 ml reaction mixture containing 4-nitrophenol

( $2 \times 10^{-5}$  M /10 ppm), photocatalyst (1 g/L), sacrificial donor TEOA ( $2 \times 10^{-4}$  M) and catalytic amount of  $\text{K}_2\text{PtCl}_4$  salt was stirred for 1h in the dark condition to attain the adsorption/de-adsorption equilibrium between the catalyst and 4-nitrophenol. Then the solution was irradiated under visible light (45 watt household CFL lamp). The photocatalysis reaction has been done in the inert atmosphere.

At a regular interval a certain amount of the aliquot was taken out, centrifuged to separate the catalyst and preserved it in the dark for further spectral analysis. The filtered catalyst was washed several times in acetonitrile and kept it for further characterization. The photoreduction reaction was investigated for 24 h.

### Sample preparation for GCMS Study

The GCMS of the reduced product was carried out by using Thermo Scientific Trace 1300 Gas Chromatography and ISQ single Quadrupole MS. After the 24 h reaction the organic solvent (MeCN) was evaporated to dryness by rotary evaporator. The dried product was dissolved in a minimum amount of acetonitrile, and it was analysed by GCMS.

### Acknowledgements

The authors, RA is grateful to SERB (DST), New Delhi for funding, and SB thanks the UGC for research fellowship. Further, the authors extend their acknowledgements to CRF-IIT-Kharagpur for SEM and EDX measurement and Department of Physics, IIT-Kharagpur for XPS data.

### Notes and References

Department of Chemistry, Green Environmental Materials & Analytical Chemistry Laboratory, Indian Institute of Technology, Kharagpur 721302, India. E-mail: raja.iitchem@yahoo.com; Fax: +91 3222-282252; Tel: +91 3222-282322

### References:

1. B. Meunier, *Science*, 2002, **296**, 270.
2. P. Sawunyama, A. Fujishima, K. Hashimoto, *Langmuir*, 1999, **15**, 3551.
3. V. Brezov, A. Blakovi, I. Surina, B. Havlfnov, *J. Photochem. Photobiol. A*, 1997, **107**, 233.
4. D. Chu, Y. Masuda, T. Ohji, K. Kato, *Langmuir*, 2010, **26**, 2811.
5. J. Zhan, H. Dong, Y. Liu, Y. Wang, Z. Chen, L. Zhang, *CrystEngComm*, 2013, **15**, 10272.
6. (a) Y. Han, X. Wu, Y. Ma, L. Gong, F. Qu, H. Fan, *CrystEngComm*, 2011, **13**, 3506; (b) G. Cheng, J. Chen, H. Ke, J. Shang, R. Chu, *Materials Lett.*, 2011, **65**, 3327.
7. (a) S. Lee, Y. Lee, D. H. Kim, J. H. Moon, *ACS Appl. Mater. Interfaces*, 2013, **5**, 12526; (b) G. Yang, Z. Jiang, H. Shi, T. Xiao, Z. Yan, *J. Mater. Chem.*, 2010, **20**, 5301; (c) B. Kraeutler, A. J. Bard, *J. Am. Chem. Soc.*, 1978, **100**, 4317.
8. E. Kowalska, H. Remita, C. Colbeau-Justin, J. Hupka, J. Belloni, *J. Phys. Chem. C*, 2008, **112**, 1124.
9. G. J. Kavarnos, N. J. Turro, *Chem. Rev.*, 1986, **86**, 401.
10. X. Pan, Y. J. Xu, *ACS Appl. Mater. Interfaces*, 2014, **6**, 1879.
11. R. A. Larson, P. L. Stackhouse, T. Crowley, *Environ. Sci. Technol.*, 1992, **26**, 1792.
12. Q. Li, Z. Peng, Y. Li, S. Li, G. Lu, *J. Phys. Chem. C*, 2007, **111**, 8237.
13. K. Whitehead, J. I. Hedges, *J. Photochem. Photobiol. B*, 2005, **80**, 115.
14. H. Cui, H. M. Hwang, S. Cook, K. Zeng, *Chemosphere*, 2001, **44**, 621.



15. W. Zhao, Y. Sun, F. Castellano, *J. Am. Chem. Soc.* 2008, **130**, 12566.
16. S. Fuldner, R. Mild, H. I. Siegmund, J. A. Schroeder, M. Gruber, B. Koenig, *Green Chem.*, 2010, **12**, 400.
- 5 17. D. Jing, L. Guo, *Catal. Commun.*, 2007, **8**, 795.
18. H. Zhang, Y. Zhou, M. Zhang, T. Shen, Y. Li, D. Zhu, *J. Colloid Interface Sci.* 2003, **264**, 290.
19. H. Park and W. Choi, *Langmuir*, 2006, **22**, 2906.
- 10 20. T. P. Chou, Q. Zhang, G. Cao, *J. Phys. Chem. C*, 2007, **111**, 18804.
21. G. C. C. Yang, S. W. Chan, *J. Nanopart. Res.*, 2009, **11**, 221.
22. S. Sarkar, A. Makhil, T. Bora, K. Lakshman, A. Singha, J. Dutta, S. K. Pal, *ACS Appl. Mater. Interfaces*, 2012, **4**, 7027.
- 15 23. Z. Zand, F. Kazemi, S. Hosseini, *Tetrahedron Lett.*, 2014, **55**, 338.
24. A. Hernández-Gordillo, A. G. Romero, F. Tzompantzi, S. Oros-Ruiz, R. Gómez, *Appl. Catal., B*, 2014, **144**, 507.
25. P. Eskandaria, F. Kazemia, Z. Zand, *J. Photochem. Photobiol., A*, 2014, **274**, 7.
- 20 26. (a) F. X. Xiao, J. Miao, B. Liu, *J. Am. Chem. Soc.*, 2014, **136**, 1559; (b) Z. Chen, S. Liu, Min-Quan Yang, Yi-Jun Xu, *ACS Appl. Mater. Interfaces*, 2013, **5**, 4309.
27. N. Gupta, B. Pal, *J. Nanosci. Nanotechnol.*, 2013, **13**, 4917.
28. Mohamed M. Mohamed, M. S. Al-Sharif, *Appl. Catal., B*, 2013, **142-143**, 432.
- 25 29. S. Gazi, R. Ananthakrishnan, *Appl. Catal., B*, 2011, **105**, 317.
30. (a) J. Warnan, V. M. Guerin, F. B. Anne, Y. Pellegrin, E. Blart, D. Jacquemin, T. Pauporté, F. Odobel, *J. Phys. Chem., C*, 2013, **117**, 8652; (b) N. Memarian, I. Concina, A. Braga, S. Md. Rozati, A. Vomiero, G. Sberveglieri, *Angew. Chem. Int. Ed.*, 2011, **50**, 12321.
31. G. Sprintschnik, H. W. Sprintschnik, P. P. Kirsch, D. G. Whitten, *J. Am. Chem. Soc.*, 1977, 4947.
- 35 32. N. Vlachopoulos, P. Liska, J. Augustynski, M. Gratzel, *J. Am. Chem. Soc.*, 1988, **110**, 1216.
33. (a) K. Westermark, H. Rensmo, K. Keis, A. Hagfeldt, L. Ojamae, P. Persson, H. Siegbahn, *J. Phys. Chem. B*, 2002, **106**, 10102; (b) R. Argazzi, C. A. Bignozzi, T. A. Heimer, F. N. Castellano, G. J. Meyer, *Inorg. Chem.*, 1994, **33**, 5741; (c) T. A. Heimer, E. J. Heilweil, *J. Phys. Chem. B*, 1997, **101**, 10990.
- 40 34. T. D. M. Bell, C. Pagba, M. Myahkostupov, J. Hofkens, P. Piotrowiak, *J. Phys. Chem. B*, 2006, **110**, 25314.
35. F. Yan, L. Huang, J. Zheng, J. Huang, Z. Lin, F. Huang, M. Wei, *Langmuir*, 2010, **26**, 7153.
- 45 36. S. K. Ghosh, M. Mandal, S. Kundu, S. Nath, T. Pal, *Appl. Catal., A*, 2004, **268**, 61.
37. S. Panigrahi, S. Basu, S. Praharaj, S. Pande, S. Jana, A. Pal, S. K. Ghosh, T. Pal, *J. Phys. Chem. C*, 2007, **111**, 4596.
- 50 38. Scavenger trapping reagent (a) C. Kormann, D. W. Bahnemann, M. Hofmann, *Environ. Sci. Technol.*, 1988, **22**, 998. (b) M. Styliidi, D. I. Konderides, X. E. Verykios, *Appl. Catal., B*, 2004, **47**, 189.
39. P. Ceroni, G. Bergamini, V. Balzani, *Angew. Chem. Int. Ed.*, 2009, **48**, 8516.
- 55 40. C. Bauer, G. Boschloo, E. Mukhtar, A. Hagfeldt, *J. Phys. Chem. B*, 2001, **105**(24), 5585; (b) K. Kalyanasundaram, N. Vlachopoulos, V. Krishnan, A. Monnier, M. Gratzel, *J. Phys. Chem.*, 1987, **91**, 2342; (c) J. B. Asbury, N. A. Anderson, E. Hao, X. Ai, T. Lian, *J. Phys. Chem. B*, 2003, **107**, 7376.
- 60 41. M. M. Maitani, C. Zhan, D. Mochizuki, E. Suzuki, Y. Wada, *Appl. Catal. B*, 2014, **147**, 770.
42. (a) V. Subramanian, E. E. Wolf, P. V. Kamat, *J. Am. Chem. Soc.*, 2004, **126**, 4943; (b) M. Jacob, H. Levanon, P. V. Kamat, *Nano Lett.*, 2003, **3**, 353.
- 65 43. R. Ananthakrishnan, S. Gazi, *Catal. Sci. Technol.*, 2012, **2**, 1463.
44. Broomhead, Young, *Inorg. Synth.*, 1992, **29**, 127.